Resonant Raman scattering and interference effects of LO phonons at the $E_0+\Delta_0$ gap of InP

Wolfgang Kauschke and Manuel Cardona
Max-Planck-Institut für Festkörperforschung, Heisenbergstrasse 1, D-7000 Stuttgart 80, Federal Republic of Germany
(Received 28 October 1985)

We have studied the resonant Raman scattering by LO and two-LO phonons and LO-phonon interference effects near the $E_0+\Delta_0$ gap of InP. Absolute values of the corresponding Raman efficiencies and Raman polarizabilities are displayed and compared with theoretical calculations. From the resonance in the two-LO-phonon scattering, the position of the $E_0+\Delta_0$ gap and its Lorentzian broadening are determined at 100 K to be 1.509 ± 0.003 eV and 5.0 ± 0.5 meV, respectively. The extrinsic impurity-induced contribution to the LO-phonon forbidden scattering is shown to play a dominant role with respect to the intrinsic q-induced mechanism even in high-purity InP. The broadening of the $E_0+\Delta_0$ gap, as obtained from the resonance in the two-LO-phonon scattering, yields an electron-phonon deformation potential $d_0=14$ eV, much smaller than usually assumed.

I. INTRODUCTION

In high-purity GaAs, forbidden Raman scattering by one LO phonon, arising from the intraband Fröhlich electron-phonon interaction, has been shown to interfere with the corresponding allowed scattering due to the deformation-potential mechanism.[1] Two contributions to the forbidden Raman scattering by LO phonons, an intrinsic q-induced one and an extrinsic impurity-induced one, could be quantitatively separated by investigating the resonance behavior of interference effects between allowed and forbidden Raman scattering by LO phonons near the $E_0+\Delta_0$ gap of GaAs.[2] The extrinsic mechanism was shown to be formally similar to the scattering by two phonons, with the impurity playing the role of one of the phonons. Resonant Raman scattering by two LO phonons has been the object of a number of investigations, particularly the recent work on $Cd_xHg_{1-x}Te$ near the $E_0+\Delta_0$ gap.[3] It is shown in this work that the peak of the resonance profile occurs when the frequency of the scattered light equals that of the corresponding gap. An analysis of the measured resonance profiles of the two LO phonons yields rather accurate values for the gap energies and their Lorentzian broadenings.

In this paper we combine both studies and investigate allowed and forbidden Raman scattering by LO phonons, Raman scattering by two LO phonons, and LO-phonon interference effects in high-purity InP near the $E_0+\Delta_0$ gap [≈ 1.51 eV at 100 K (Refs. 4 and 5)]. We demonstrate the generality of the interference phenomenon between allowed and forbidden Raman scattering by LO phonons by reporting its observation for InP. We also analyze the resonance obtained for two-LO-phonon scattering and determine from these results the position and the Lorentzian broadening of the $E_0+\Delta_0$ gap. From an analysis of this broadening we obtain the deformation potential $d_0\approx 14$ eV for the coupling of the Γ_{15} valence-band states to LO phonons.

II. THEORY

The Raman scattering efficiency $dS/d\Omega$ (per unit length and unit solid angle Ω) is used to compare LO-phonon forbidden and two-LO-phonon Raman scattering, while the first-order Raman tensor $\overleftrightarrow{R}$ and its independent components, the Raman polarizabilities a, are convenient to display the intensity of LO-phonon allowed and forbidden Raman scattering.

The efficiency $(dS/d\Omega)_{LO}$ of Raman scattering by LO phonons can be written as a function of the Raman tensor:[2]

$$\left[\frac{dS}{d\Omega}\right]_{LO}=\frac{\omega_S^3\omega_L}{c^4}\frac{\hbar}{2V_cM^*\Omega_{LO}}\frac{n_S}{n_L}\,|\hat{\mathbf{e}}_S\cdot\overleftrightarrow{R}\cdot\hat{\mathbf{e}}_L|^2 \times[1+n(\Omega_{LO})]\,, \tag{1}$$

where ω_L (ω_S) is the frequency of the incident (scattered) photon, c is the speed of light in vacuum, V_c the volume of the primitive cell, $M^*=(M_{In}^{-1}+M_P^{-1})^{-1}$ the reduced mass of the unit cell, Ω_{LO} the frequency of the LO phonon, $n(\Omega_{LO})$ the LO-phonon occupation number, n_L (n_S) the refractive index, and $\hat{\mathbf{e}}_L$ ($\hat{\mathbf{e}}_S$) the polarization vector of the incident (scattered) light. A similar expression holds for the efficiency $(dS/d\Omega)_{2LO}$ of Raman scattering by two LO phonons as given by Eqs. (2) and (7) of Ref. 3.

The Raman scattering efficiencies $(dS/d\Omega)_{LO}$ and $(dS/d\Omega)_{2LO}$ can be related to the measured scattering rate R_S' *outside* the crystal by[2]

$$R_S'=\left[\frac{T_LT_SP_L'}{(\alpha_L+\alpha_S)n_S^2\hbar\omega_L}\right]\Delta\Omega'\frac{dS}{d\Omega}\,. \tag{2}$$

Here, T_L (T_S) is the power-transmission coefficient of the incident (scattered) light defined by $T=1-r$, where r is the reflectivity, and P_L' is the power of the light incident on the sample. α_L (α_S) is the absorption coeffi-

cient of the incident (scattered) light and $\Delta\Omega'$ the solid angle for collection outside the crystal. The large parentheses in Eq. (2) must be used to correct the measured scattering rates in order to obtain scattering efficiencies. An expression relating the measured scattering rate R_S' to the square of the appropriate component of the Raman tensor $|\hat{\mathbf{e}}_S\cdot\vec{\mathbf{R}}\cdot\hat{\mathbf{e}}_L|^2$ can be derived from Eqs. (1) and (2) and is given explicitly by Eq. (6) of Ref. 2.

The allowed Raman scattering by LO phonons occurs via deformation-potential (DP) electron-phonon interaction. For backscattering at a (001) face the Raman tensor is given by[6]

$$\vec{\mathbf{R}}_{\mathrm{DP}}=\begin{bmatrix}0 & a_{\mathrm{DP}} & 0\\ a_{\mathrm{DP}} & 0 & 0\\ 0 & 0 & 0\end{bmatrix}. \tag{3}$$

The deformation-potential-induced Raman polarizability a_{DP} can be written in terms of contributions of the critical points $E_0-E_0+\Delta_0(A_1)$, $E_1-E_1+\Delta_1(A_2)$, and higher gaps (A_3):[6]

$$a_{\mathrm{DP}}=A_1\left\{\frac{2E_0[f(x_0-\hbar\Omega_{\mathrm{LO}}/2E_0)-f(x_0+\hbar\Omega_{\mathrm{LO}}/2E_0)]}{\hbar\Omega_{\mathrm{LO}}}+\frac{4E_0}{\Delta_0}\left[f(x_0)-\left[\frac{E_0}{E_0+\Delta_0}\right]^{3/2}f(x_{0s})\right]\right\}+A_2\left[\frac{1}{1-x_1^2}+\left[\frac{E_1}{E_1+\Delta_1}\right]^2\frac{1}{1-x_{1s}^2}\right]+A_3\ , \tag{4}$$

with

$$f(x)=x^{-2}[2-(1+x)^{1/2}-(1-x)^{1/2}]\ .$$

The x variables are "reduced" energies defined as $x_0=\hbar\omega_L/E_0$, $x_{0s}=\hbar\omega_L/E_0+\Delta_0$, $x_1=\hbar\omega_L/E_1$, and $x_{1s}=\hbar\omega_L/E_1+\Delta_1$. Equation (4) corresponds to Eq. (8) of Ref. 6 with the derivative $g(x_0)$ replaced by the finite difference of f functions.[7] Near $E_0+\Delta_0$ this change has to be made for semiconductors in which the spin-orbit splitting Δ_0 [$\approx$100 meV in InP (Ref. 5)] is not much larger than the phonon energy $\hbar\Omega_{\mathrm{LO}}$ [$\approx$43 meV in InP (Ref. 8)].

The allowed Raman scattering by optical phonons reveals a strong resonance at the critical points E_0 and E_1. However, the dispersion should be weak at the $E_0+\Delta_0$ gap [e.g., the measurements for TO phonons in InP (Ref. 9) and GaAs (Ref. 6) and for LO phonons in GaAs (Ref. 1)], except in cases where the excitonic exchange interaction is large.[10] The factors A_1 and A_2 (usually given in units of Å^2) can be related to the first-order optical deformation potential d_0 of the $E_0+\Delta_0$ gap and to the three-band deformation potential $d_{3,0}^5$ of the $E_1-E_1+\Delta_1$ gap through[6]

$$A_1=\frac{\sqrt{3}}{128\pi}\frac{a_0^2}{E_0}C_0''d_0 \tag{5}$$

and

$$A_2=0.72\frac{a_0}{E_1^2}d_{3,0}^5\ . \tag{6}$$

a_0 is the lattice constant and C_0'' is a constant which determines the contributions of the E_0 and $E_0+\Delta_0$ gaps ($E_0\gg\Delta_0$) to the dielectric function ϵ:[6,11]

$$\Delta\epsilon=C_0''[f(x_0)+0.435f(x_{0s})]\ . \tag{7}$$

The constant C_0'' can be obtained from the birefringence induced by a [111] stress (same symmetry as the optical phonon), but unfortunately with a large uncertainty.[12] Since $C_0''\propto P^{-1}$ holds (P is the interband matrix element of linear momentum),[11] C_0'' should not vary much from GaAs to InP.[6] The factors A_1, A_2, and A_3 can also be viewed as disposable parameters to fit the experimental scattering efficiencies.

Forbidden Raman scattering by LO phonons involves two mechanisms: an intrinsic $\mathbf{q}$-induced one via the electric field which accompanies the LO phonon (Fröhlich interaction), leading to the same final states as the deformation-potential-induced Raman scattering (coherent), and an extrinsic one, via Fröhlich electron-phonon and electron-impurity interaction, leading to a manifold of different states with different wave vectors $\mathbf{q}$ (incoherent). An additional mechanism exists in the presence of a strong dc electric field.[7] It will not be discussed here since such a field is not present in our experiments.

The intrinsic LO-phonon forbidden Raman scattering arises from intraband matrix elements of the Fröhlich interaction when one takes the $\mathbf{q}$ dependence of these matrix elements into account. For the $E_0+\Delta_0$ gap the Raman tensor $\vec{\mathbf{R}}_F$ is a diagonal tensor:[2]

$$\vec{\mathbf{R}}_F=\begin{bmatrix}a_F & 0 & 0\\ 0 & a_F & 0\\ 0 & 0 & a_F\end{bmatrix}. \tag{8}$$

For the case of transitions between uncorrelated electrons (no excitonic effects) the $\mathbf{q}$-induced Raman polarizability a_F can be written as[2]

$$a_F=\frac{q}{12\pi}\left[\frac{e}{m\hbar}\right]^2\frac{C_F}{\hbar\Omega_{\mathrm{LO}}}\left[\frac{1}{\omega_L}\right]^2\left[\frac{\omega_L}{\omega_S}\right]^{1/2}\times(4V_c\mu M^*)^{1/2}\frac{2P^2}{3}(s_e-s_h)F(\omega_L)\ , \tag{9}$$

with

$$F(\omega)=\left[\left|\frac{\hbar\omega-E_0-\Delta_0+i\eta}{\hbar\Omega_{\mathrm{LO}}}\right|^{1/2}-\left|\frac{\hbar\omega-\hbar\Omega_{\mathrm{LO}}-E_0-\Delta_0+i\eta}{\hbar\Omega_{\mathrm{LO}}}\right|^{1/2}\right]^3 .$$

In Eq. (9) $\mathbf{q}$ is the wave vector of the created phonon, e and m are the free-electron charge and mass, respectively, $\mu^{-1}=m_e^{-1}+m_h^{-1}$, and $s_{e,h}=m_{e,h}/(m_e+m_h)$, where m_e (m_h) is the effective electron (hole) mass. The Fröhlich constant C_F is given by

$$C_F=[2\pi e^2(1/\epsilon_\infty-1/\epsilon_0)\hbar\Omega_{\mathrm{LO}}]^{1/2}=\frac{e_{\mathrm{T}}e}{\epsilon_\infty}\left|\frac{8\pi^2\hbar}{V_c M^*\Omega_{\mathrm{LO}}}\right|^{1/2}, \quad (10)$$

ϵ_0 and ϵ_∞ being the low- (rf) and high-frequency (ir) dielectric constant, and e_{T} the transverse dynamical charge. The definition of the function F implies the convention that the imaginary parts of the square roots are positive. η describes the broadening of the $E_0+\Delta_0$ gap.

The intrinsic forbidden Raman scattering by LO phonons resonates between $E_0+\Delta_0$ and $E_0+\Delta_0+\hbar\Omega_{\mathrm{LO}}$ with a maximum around $E_0+\Delta_0+\hbar\Omega_{\mathrm{LO}}/2$. The resonance line shape does not vary sensitively with the broadening η of the $E_0+\Delta_0$ gap, since only single resonances occur. We show in Fig. 1 the results of a calculation with Eq. (9) using the parameters appropriate to InP (Table I) for five different values of η (0, 1, 2, 5, and 8 meV). Note that for $\eta=0$ the resonance profile reveals a plateau with square-root singularities at its corners separated by the energy $\hbar\Omega_{\mathrm{LO}}$ of the LO phonon. For η much smaller than $\hbar\Omega_{\mathrm{LO}}$ the profile approaches rapidly that for $\eta=0$. Hence, in this case it becomes rather difficult to extract the broadening η from the shape or the width of the resonance.

The existence of extrinsic impurity-induced forbidden Raman scattering by LO phonons was suggested by several authors.[13] It can be evaluated in fourth-order perturbation theory.[2] In spite of this, its scattering efficiency becomes comparable with that of the intrinsic LO-phonon forbidden Raman scattering, since the momentum conservation is relaxed in this process. Larger $\mathbf{q}$ vectors enhance the scattering efficiency ($\propto q^2$) and double resonances occur at $E_0+\Delta_0+\hbar\Omega_{\mathrm{LO}}$ (outgoing resonance) which are quite sensitive to the broadening η of the $E_0+\Delta_0$ gap. The Raman tensor $\overleftrightarrow{R}_{Fi}$ for impurity-induced LO-phonon forbidden Raman scattering near $E_0+\Delta_0$ is diagonal. The square $|a_{Fi}|^2$ of the Raman polarizability and other details of the calculations, assuming scattering by ionized impurities, are given in Ref. 2 [Eq. (A1)].

Figure 2 displays the results of a calculation with Eq. (A1) of Ref. 2 using the parameters appropriate to InP (Table I) for three different values of η (2, 5, and 8 meV).

TABLE I. Parameters used to evaluate the theoretical expressions of the Raman polarizabilities in InP.

$E_0=1.41$ eV[a]	$E_1=3.15$ eV[c]
$E_0+\Delta_0=(1.509\pm0.003)$ eV[b]	$E_1+\Delta_1=3.28$ eV[c]
$\eta=(5.0\pm0.5)$ meV	$\hbar\Omega_{\mathrm{LO}}=43$ meV[d]
$m_e=0.077m$[e]	$M^*=44\,782m$
$m_h=0.21m$[f]	$a_0=5.8725$ Å[g]
$P^2/m\simeq8.7$ eV[h]	$C_F=3.07\times10^{-5}$ eV cm$^{1/2}$[i]
$q=5.3\times10^5$ cm^{-1}[j]	$X_F=0.06$[k]

[a]Reference 4.
[b]Value used for the fit of the two-LO-phonon resonance profile (see text).
[c]Reference 41.
[d]$\Omega_{\mathrm{LO}}=347$ cm^{-1} at 100 K (Ref. 8).
[e]Reference 42.
[f]Reference 43.
[g]Reference 44.
[h]$P\approx2\pi/a_0$.
[i]See Eq. (10) and Ref. 45.
[j]$q=(n_L\omega_L+n_S\omega_S)/c$.
[k]See definition in Ref. 2.

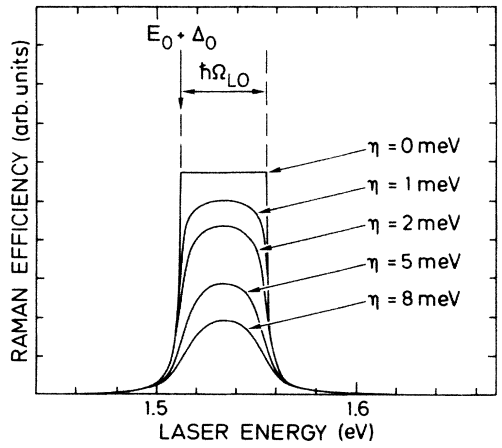

FIG. 1. Raman efficiency for intrinsic q-induced forbidden scattering by one LO phonon calculated with Eq. (9) using the parameters appropriate to InP (Table I) for five different values of η (0, 1, 2, 5, and 8 meV).

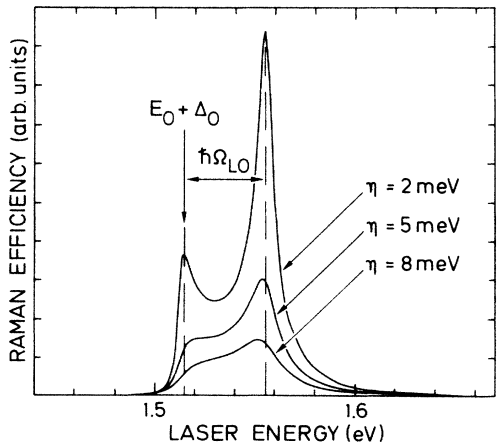

FIG. 2. Raman efficiency for extrinsic impurity-induced forbidden scattering by one LO phonon calculated with Eq. (A1) of Ref. 2 using the parameters appropriate to InP (Table I) for three different values of η (2, 5, and 8 meV).

Note that for $\eta \approx 0$ the resonance profile seems to diverge at $E_0+\Delta_0$ (ingoing resonance) and $E_0+\Delta_0+\hbar\Omega_{LO}$ (outgoing resonance), preventing a numerical evaluation of the integral in Eq. (A1) of Ref. 2. For η much smaller than $\hbar\Omega_{LO}$ the profile reveals two peaks separated by the energy $\hbar\Omega_{LO}$ of the LO phonon, the stronger one at the outgoing resonance. Hence, for small broadenings η and a dominant contribution of the impurity-induced mechanism to the forbidden Raman scattering by LO phonons, the resonance shows a sharp feature at the outgoing resonance which allows an evaluation of the $E_0+\Delta_0$ gap position and its Lorentzian broadening η. However, in the case of larger broadenings or higher contributions of intrinsic forbidden Raman scattering by LO phonons, the resonance profile smears out and a determination of the $E_0+\Delta_0$ gap position and its broadening from the shape or the width of the resonance becomes rather difficult.

Two-LO-phonon Raman scattering by intraband Fröhlich interaction is isomorphic to the impurity-induced LO-phonon forbidden Raman scattering, with the electron-impurity Coulomb interaction replaced by the Fröhlich interaction. Thus, the calculations of Refs. 14–18 and 3 lead, also in this case, to a diagonal tensor. An expression for the two-LO-phonon Raman scattering efficiency $(dS/d\Omega)_{2LO}$ is given by Eqs. (2) and (7) of Ref. 3. Double resonances occur at $E_0+\Delta_0+2\hbar\Omega_{LO}$ (outgoing resonance), the resonance maximum varying sensitively with the broadening η of the $E_0+\Delta_0$ gap. We show in Fig. 3 the result of calculations performed with Eqs. (2) and (7) of Ref. 3 using the parameters appropriate to InP (Table I) for three different values of η (2, 5, and 8 meV). Note that the *apparent* broadenings of the resonance profiles, with only one peak at the outgoing resonance ($E_0+\Delta_0+2\hbar\Omega_{LO}$), are not only determined by the Lorentzian broadening η of the $E_0+\Delta_0$ gap, but also by the energy $\hbar\Omega_{LO}$ of the LO phonon. The maxima of the scattering efficiency are inversely proportional to the square of the apparent width of the resonance profiles. A numerical evaluation of the integral according to Eq. (7) of Ref. 3 becomes impossible in the limit of negligibly small η, as in the case of impurity-induced scattering by LO phonons (see above). Hence, we cannot say with certainty whether for $\eta \to 0$ the apparent width tends to zero and whether the resonance maximum diverges. According to our calculations for $\eta \geqq 1$ meV the resonance profile for two-LO-phonon Raman scattering, revealing only one peak at the outgoing resonance, allows one to determine accurately the position and the broadening of the $E_0+\Delta_0$ gap.

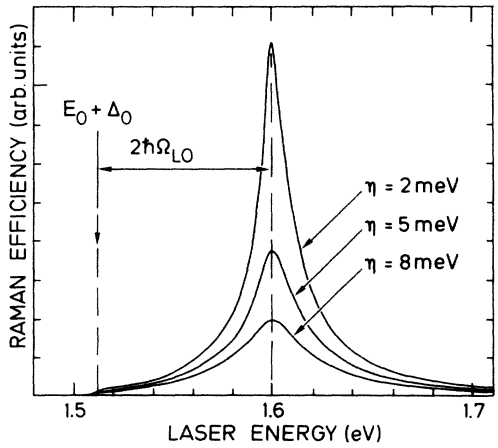

FIG. 3. Raman efficiency for scattering by two LO phonons calculated with Eqs. (2) and (7) of Ref. 3 using the parameters appropriate to InP (Table I) for three different values of η (2, 5, and 8 meV).

The broadening parameter η can be related to the optical deformation potential d_0 following the analysis of Lawaetz.[19] The basic assumption is that the broadening of the $E_0+\Delta_0$ gap is essentially determined by the lifetime of the hole in the split-off band. At low temperature the hole state in the split-off band decays into the heavy-hole and light-hole bands through emission of an optical phonon. Neglecting multipole coupling of phonons to electrons, there are two contributions to the broadening η of the $E_0+\Delta_0$ gap [Eqs. (5-29) and (5-31) of Ref. 19]:

$$\eta \approx \zeta_1 d_0^2 + \zeta_p a_p^2 . \tag{11}$$

$\zeta_1 d_0^2$ describes the broadening by nonpolar deformation-potential interaction and ζ_1 is a weighting factor which takes the density of states and the **k**-space integration into account ($\zeta_1 = 5\times10^{-6}$ eV^{-1} was evaluated for InP in Ref. 19). $\zeta_p a_p^2$ yields the polar contribution, a_p describes the strength of the polar-optical coupling, and ζ_p is a weighting factor similar to ζ_1. The polar contribution $\zeta_p a_p^2$ to the broadening η amounts to 4 meV in InP.[19] The deformation-potential contribution $\zeta_1 d_0^2$ is calculated to be 6 meV,[19] with the value of $d_0 = 35$ eV, which is obtained theoretically with the non-self-consistent empirical pseudopotential method (EPM).[20]

Our analysis of LO-phonon interference effects is based on the fact that the Raman tensors for LO-phonon allowed and intrinsic forbidden Raman scattering should be (coherently) added *before* squaring [Eqs. (3) and (8)], while the extrinsic LO-phonon forbidden scattering should be (incoherently) added *after* squaring. We denote by **x**, **y**, **z**, **x'**, and **y'** the [100], [010], [001], [110], and [1$\bar{1}$0] directions of the crystal, respectively. The [110] and [1$\bar{1}$0] directions are physically inequivalent in III-V compounds. However, the labeling depends on the choice of the coordinates. With the earlier convention [the In atoms at (0,0,0), the P atoms at $(a_0/4)(1,1,1)$ (Ref. 2)], the ($\bar{1}\bar{1}$) face, parallel to [110], is In-terminated.

We used four backscattering configurations at a (001) face in order to measure LO-phonon interference effects (I and II), LO-phonon forbidden Raman scattering (III), and LO-phonon allowed Raman scattering (IV). The square $|\hat{\mathbf{e}}_S \cdot \vec{\mathbf{R}} \cdot \hat{\mathbf{e}}_L|^2$ of the Raman tensor in the four scattering geometries amounts to

$$\begin{aligned}
&\text{(I)}\ \mathbf{z}(\mathbf{x}',\mathbf{x}')\bar{\mathbf{z}}\text{:}\quad |a_F + a_{DP}|^2 + |a_{Fi}|^2 ,\\
&\text{(II)}\ \mathbf{z}(\mathbf{y}',\mathbf{y}')\bar{\mathbf{z}}\text{:}\quad |a_F - a_{DP}|^2 + |a_{Fi}|^2 ,\\
&\text{(III)}\ \mathbf{z}(\mathbf{x},\mathbf{x})\bar{\mathbf{z}}\text{:}\quad |a_F|^2 + |a_{Fi}|^2 ,\\
&\text{(IV)}\ \mathbf{z}(\mathbf{y},\mathbf{x})\bar{\mathbf{z}}\text{:}\quad |a_{DP}|^2 .
\end{aligned} \tag{12}$$

We have investigated the Raman scattering by two LO

phonons in configuration III. Configurations I and II should give the same results as configuration III.

III. EXPERIMENTAL DETAILS

The samples studied were two n-type undoped epitaxial layers ($d \approx 1.5$ μm) of InP grown on semi-insulating InP:Fe(001) substrates by the MOCVD (metal-organic chemical-vapor-deposition) technique. Sample 1 was supplied by M. Heyen and H. Jürgensen, University of Aachen, while sample 2 was obtained from K. Benz and F. Scholz, University of Stuttgart. Electrical measurements at 77 K yield the carrier concentrations $n_{77} \approx 1 \times 10^{15}$ cm^{-3} (sample 1) and $n_{77} \approx 1.4 \times 10^{15}$ cm^{-3} (sample 2). The growers of sample 2 reported to us a mobility $\mu_{77} = 45\,500$ cm^2/V s. The [110] and [1$\bar{1}$0] directions were determined by inspection of the etch pattern. Preferential etching of the (001) face with a $0.6N$ solution of Fe^{3+} ions in HCl (36 mol%) produces a rectangular pyramidal structure, the four sides being {111} planes.[21] Since In-terminated faces are less reactive than P-terminated ones, In-terminated {111} planes develop more easily. This means that the longest sides of the pyramids are parallel to [110].[21,22] This effect allows the orientation of the sample to be determined.

The Raman measurements were performed with a cw dye laser using the normal and infrared-extended version of the dye LD700 (Lambda Physik, Göttingen). This dye was pumped with all red lines of a Kr^+ laser (4.5 W). It lased in the frequency range 1.5–1.7 eV, close to the $E_0 + \Delta_0$ gap of InP. The laser beam was focused onto the sample with a cylindrical lens. The power density was kept below 10 W/cm^2.

Three similar samples were cut and mounted next to each other in a liquid-nitrogen cryostat in such a way that the measurements in the $\mathbf{z}(\mathbf{x}',\mathbf{x}')\bar{\mathbf{z}}$, $\mathbf{z}(\mathbf{y}',\mathbf{y}')\bar{\mathbf{z}}$, and $\mathbf{z}(\mathbf{x},\mathbf{x})\bar{\mathbf{z}}$ configurations could be performed without changing the polarization of the incident and scattered light simply by means of a parallel translation of the samples with respect to the entrance slit of the monochromator. The polarization of the incident light was changed for the measurement of allowed Raman scattering by LO phonons in the $\mathbf{z}(\mathbf{y},\mathbf{x})\bar{\mathbf{z}}$ configuration.

In order to obtain absolute values for the Raman scattering efficiencies and the Raman tensor, we used the sample-substitution method.[7] We chose high-purity silicon as a reference. Its Raman tensor is known to show low dispersion within the frequency range under investigation. For the Raman polarizability $|a|$ of the optical phonon of Si, we use 30 Å^2 at $\hbar\omega_L \approx 1.6$ eV corresponding to the Raman scattering efficiency $dS/d\Omega = 2.2 \times 10^{-6}$ sr^{-1}cm^{-1}.[23] The experimental scattering rates R_S' outside the crystal were obtained from the area of the optical-phonon lines measured for InP and Si, respectively. These data were corrected for absorption, reflectivity, and the refractive index according to Eq. (2) for the scattering efficiency $dS/d\Omega$ and according to Eq. (6) of Ref. 2 for $|\hat{\mathbf{e}}_S \cdot \vec{\mathbf{R}} \cdot \hat{\mathbf{e}}_L|^2$. The absorption data for Si were taken from Dash and Newman.[24] For InP no absorption coefficients are available within the frequency range 1.5–1.7 eV. We thus interpolated between the values obtained by Turner *et al.*[4] near the absorption edge (≈ 1.4 eV) at 77 K and data determined by ellipsometry ($\hbar\omega_L > 2.0$ eV) by Aspnes and Studna[25] at room temperature, shifting the latter by 80 meV (Ref. 4) so as to simulate low-temperature data. Additional data for the transmission coefficients and the refractive indices of InP and Si were taken from Ref. 25 after correcting for the temperature shift.

IV. RESULTS

Our figures will only show the experimental data of sample 1. However, the values obtained from the fit will be given for both samples. The experimental error in the measurement of the ratio of the Raman scattering efficiency of InP to that of Si obtained from the areas under the phonon lines is estimated to be about 20%.

Figure 4 displays the measured integrated scattering efficiencies $(dS/d\Omega)_{LO}$ and $(dS/d\Omega)_{2LO}$ for LO-phonon forbidden and for two-LO-phonon Raman scattering. While the Raman scattering by two LO phonons reveals a sharp resonance with only one peak, the resonance profile of the forbidden scattering by LO phonons is broad, displaying a flat plateau with corners separated approximately by the LO-phonon frequency. We give in Fig. 5 the measured values of the square $|\hat{\mathbf{e}}_S \cdot \vec{\mathbf{R}} \cdot \hat{\mathbf{e}}_L|^2$ of the Raman tensor for LO-phonon scattering in the three polarization configurations for which $\hat{\mathbf{e}}_L \| \hat{\mathbf{e}}_S$. The resonance behavior for the $\mathbf{z}(\mathbf{x}',\mathbf{x}')\bar{\mathbf{z}}$ configuration differs from that for the $\mathbf{z}(\mathbf{y}',\mathbf{y}')\bar{\mathbf{z}}$ configuration, thus confirming that a part of the LO-phonon forbidden scattering interferes with the allowed contribution. Figure 6 shows the resonance curve for the configuration $\mathbf{z}(\mathbf{y},\mathbf{x})\bar{\mathbf{z}}$ in which only allowed Raman scattering by LO phonons should be observed. In the region of Fig. 6, which includes $E_0 + \Delta_0$ but not E_0, no sharp structure should appear.[7] Nevertheless, a strong enhancement is observed toward the low-energy boundary of the laser range (see next section).

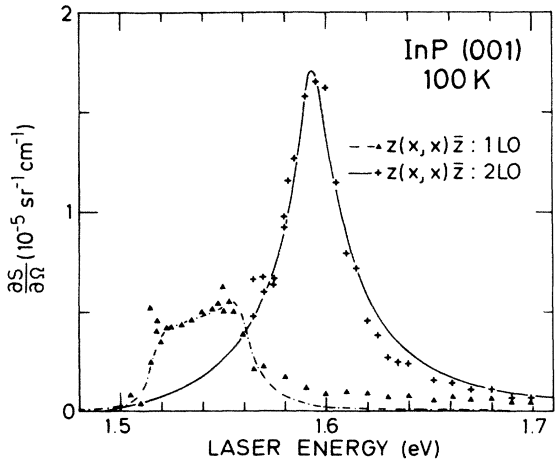

FIG. 4. Raman scattering efficiencies for LO-phonon forbidden and two-LO-phonon scattering near the $E_0 + \Delta_0$ gap of InP at $T \approx 100$ K. The lines represent fits to the experimental points.

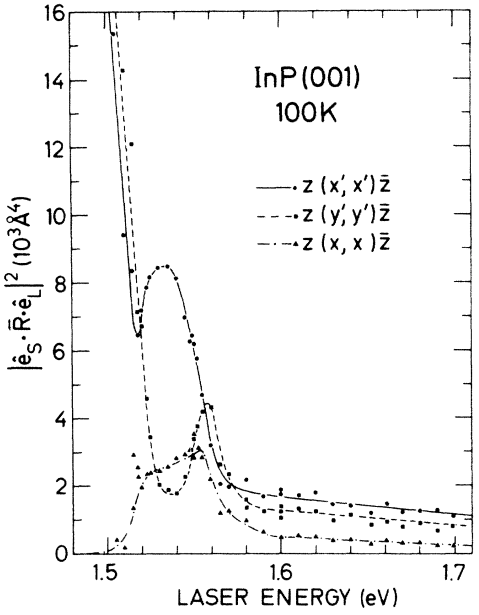

FIG. 5. LO-phonon Raman polarizabilities for the three scattering configurations ($\hat{e}_L \| \hat{e}_S$) near the $E_0+\Delta_0$ gap of InP at $T \approx 100$ K. The lines are drawn as a guide to the eye.

V. DISCUSSION

By fitting the two-LO-phonon resonance with Eqs. (2) and (7) of Ref. 3 (solid line in Fig. 4), we determine the $E_0+\Delta_0$ gap position (1.506±0.003 eV for sample 1, 1.509±0.003 eV for sample 2) and its broadening η (5.0±0.5 meV for both samples). Details concerning the fitting parameters are given in Table I.

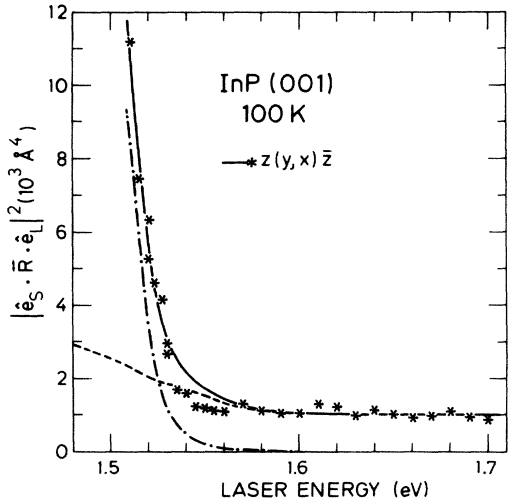

FIG. 6. Raman polarizabilities for LO-phonon allowed scattering near the $E_0+\Delta_0$ gap of InP at $T \approx 100$ K. The solid line represents the fit to the experimental resonance curve assuming a contribution from deformation-potential scattering (dashed line) and a contribution due to a further resonance of unknown origin (dotted-dashed line).

The measured Raman scattering efficiency at the maximum of the resonance [$(dS/d\Omega)_{2LO}=1.7\times10^{-5}$ $sr^{-1}cm^{-1}$] differs by a factor of 3 from the theoretical value [$(dS/d\Omega)_{2LO}=0.57\times10^{-5}$ $sr^{-1}cm^{-1}$]. The qualitative agreement is satisfactory, taking into account the total error of the Raman scattering efficiency of InP [about 50%, determined mainly by the uncertainty of the Raman scattering efficiency of Si (Ref. 23)] and considerable uncertainties of the parameters of the calculation (see Table I), which, anyway, does not include electron-hole correlation (excitonic interaction). The gap position agrees with other optical measurements [$E_0+\Delta_0=1.5$ eV at 100 K (Refs. 4 and 5)]. The broadening $\eta=5$ meV yields $d_0=14.2$ eV from Eq. (11), if we assume that the polar contribution to the broadening amounts to 4 meV.[19] This means that the essential contribution to the broadening of the $E_0+\Delta_0$ gap originates from the polar-optical coupling (4 meV) and not from the deformation-potential coupling (1 meV). Our result ($\eta=5$ meV, $d_0=14$ eV) differs dramatically from that of Lawaetz [$d_0=35$ eV (Ref. 19)], assuming $\eta=10$ meV,[26] and from the calculation using the EPM method [$d_0=35$ eV (Ref. 20)]. This discrepancy will be discussed later.

In order to fit the resonance profile of the allowed Raman scattering by LO phonons near $E_0+\Delta_0$ (Fig. 6), the strong resonance tail at lower energies ($\hbar\omega_L < 1.55$ eV) has to be removed. No successful fit can be otherwise obtained with Eq. (4). We therefore postulate that this tail is due to another mechanism. Hot luminescence is discarded as the tail is only seen for some configurations (not in the LO-phonon forbidden Raman scattering configuration). The origin of this resonance remains unknown. The observation of forbidden LO-phonon and two-LO-phonon Raman scattering becomes impossible for $\hbar\omega_S \leqq 1.49$ eV as well as the measurement of LO-phonon allowed Raman scattering for $\hbar\omega_S \leqq 1.46$ eV, since a strong luminescence due to the E_0 gap masks this energy region. Measurements at different temperatures and the investigation of Raman scattering by TO phonons for other sample orientations may provide further information.

The strong resonance for $\hbar\omega_L < 1.55$ eV has been removed, somewhat arbitrarily, by fitting it to the function $A/[(\omega_L-\omega_g)^2-\Gamma^2]^2$ and subtracting this fitted curve from the observed scattering efficiencies. The best fit is obtained for $A=1.16\times10^{-3}$, $\hbar\omega_g=1.505$ eV, and $\hbar\Gamma=18$ meV. The corresponding function is shown as the dotted-dashed line in Fig. 6. We note that the remainder of this discussion does not depend appreciably on the assumptions made for the subtraction of the low-energy tail. After removing this unidentified resonance, the remaining curve has been fitted with the sum of contributions to the allowed Raman scattering by LO phonons due to the E_0, $E_0+\Delta_0$, E_1, $E_1+\Delta_1$, and higher, gaps, according to Eq. (4). From this fit and choosing the signs of A_1, A_2, and A_3 to be the same as in GaAs, we obtain $A_1=2.2$, $A_2=15.5$, and $A_3=-3.1$ (in units of $Å^2$). The dashed line in Fig. 6 displays the fit with Eq. (4); the solid line represents the sum of the dashed and dotted-dashed lines. The deviation of the solid line in Fig. 6 from the experimental points suggests that $A_1(d_0)$ may have to be decreased in order to improve the fit. Howev-

er, the $E_0-E_0+\Delta_0$ gap contribution is the only one to yield an imaginary component of a_{DP}. Such a component is necessary to explain the interference effect of Fig. 5. The fit of Fig. 6 and the values of A_1, A_2, and A_3 represent the "best" compromise between a "good" fit of the resonance in the allowed Raman scattering by LO phonons, a "reasonable" deformation potential d_0, and a fit of the interference curves of Fig. 5.

Substituting $A_1=2.2$ into Eq. (5), we obtain an optical deformation potential d_0 between 8.4 and 11.6 eV, assuming that the value of C_0'' lies between 1.8 and 2.5, as obtained from stress-induced birefringence.[12] For $C_0''=1.5$, the best value found for GaAs,[6] d_0 becomes 13.9 eV. The factor $A_2=15.5$ yields, when replaced into Eq. (6), $d_{3,0}^5=36.4$ eV, in agreement with a relative determination of $d_{3,0}^5$ for InP, with respect to that of GaAs by TO-phonon resonance Raman scattering near the E_1 gap [$d_{3,0}^5$(GaAs)/$d_{3,0}^5$(InP) ≈ 1 (Ref. 9)] and with the values $|d_{3,0}^5|=37$ eV determined experimentally[6] and $d_{3,0}^5=35$ eV calculated recently[27] for GaAs.

The values of d_0 used for the fit of Fig. 6 are comparable to those obtained here from the broadening η of the $E_0+\Delta_0$ gap. In the contrast, an optical deformation potential d_0 between 10 and 15 eV differs strikingly from earlier experimental and theoretical values, i.e., $d_0=35.4$ eV obtained from the width of the $E_0+\Delta_0$ exciton[19,28] and $d_0=35.6$ eV from non-self-consistent calculations performed with the empirical pseudopotential method.[20] However, recent *ab initio* self-consistent calculations with the linear muffin-tin orbital (LMTO) method give $d_0=14$ eV,[29,30] in rather good agreement with the values reported here.

An inconsistency similar to that described above has also been observed in CdTe. The broadening η of the $E_0+\Delta_0$ gap has been determined by reflection spectroscopy to be 16 meV.[19,31] In contrast, the best fit of the two-LO-phonon Raman resonance was obtained for $\eta=6$ meV.[3] While a broadening $\eta=16$ meV yields an optical deformation potential $d_0=22$ eV, $\eta=6$ meV would give $d_0=11.6$ eV.[19] The LMTO method yields, for this material, $d_0=6$ eV,[30] a value also much smaller than that found with the EPM method (23 eV).[20] A similar discrepancy between EPM and LMTO calculations of d_0 also exists for Si [$d_0=35$ eV (Ref. 20), $d_0=22$ eV (Ref. 32)] and GaAs [$d_0=36$ eV (Ref. 20), $d_0=18$ eV (Ref. 29)], while a self-consistent pseudopotential calculation yields 23 eV for GaAs.[33] The broadening $\eta=8$ meV of the $E_0+\Delta_0$ gap in GaAs, which corresponds to $d_0=36$ eV,[19] has been determined by fitting the LO-phonon interferences.[2] This procedure, however, is much less sensitive to the broadening than the fit of the two-LO-phonon resonance line shape, since the apparent width of LO-phonon forbidden resonance is mainly determined by the LO-phonon frequency (see Fig. 1). Nevertheless, a broadening of 8 meV seems to be in agreement with values from other optical measurements: 10 meV from reflectance,[34] 11 meV from magnetoreflectance,[35] and 6 ± 2 meV from electroreflectance.[36] However, recent measurements on GaAs, including the two-LO-phonon resonance curve, indicate that the fits have to be revised, yielding a lower broadening parameter $\eta=3.5$ meV and an optical deformation potential $d_0=20$ eV.[37,19] Note that the broadening η of the $E_0+\Delta_0$ gap obtained from the two-LO-phonon Raman scattering is always lower than that determined by other optical methods. The deformation potentials d_0 envisaged here are, by a factor of 2 or 3, smaller than earlier ones (see, e.g., Ref. 19). An explanation of the discrepancy is lacking and will be investigated further. The possibility that excitonic effects, not included in our analysis, may lead to a sharpening of the two-phonon resonances, and thus to an apparent lowering of η, cannot be ruled out. In this case, the discrepancy between the various theoretical evaluations of d_0 would still have to be accounted for.

The experimental points in Fig. 7 were obtained from Fig. 5 by subtracting the function $A/[(\omega_L-\omega_g)^2+\Gamma^2]^2$ as discussed above. There is a large uncertainty on the lowest-energy end of the resonance curves (below 1.52 eV) which, however, does not affect the region of strong interference (≈ 1.54 eV). Having determined the position and the broadening η of the $E_0+\Delta_0$ gap, as well as the resonance behavior of a_{DP}, the LO-phonon forbidden Raman scattering [$\mathbf{z}(\mathbf{x},\mathbf{x})\bar{\mathbf{z}}$] can be fitted by means of Eq. (9) of this paper and Eq. (A1) of Ref. 2, by adjusting at the same time the height of the LO-phonon interference curves [$\mathbf{z}(\mathbf{x}',\mathbf{x}')\bar{\mathbf{z}}$ and $\mathbf{z}(\mathbf{y}',\mathbf{y}')\bar{\mathbf{z}}$] according to Eq. (11). The best fit for the allowed and forbidden Raman scattering is obtained with $E_0+\Delta_0$ 9 meV higher than the value used for the two-LO-phonon Raman scattering (1.515±0.003 eV for sample 1, 1.518±0.003 eV for sample 2, $\eta=5$ meV for both samples). For the best representation of the data the relative strength $|a_{F,\max}/a_{Fi,\max}|^2$ of the intrinsic and extrinsic forbidden Raman scattering by one LO phonon at the maximum of the resonance profile must be taken to be 40±5%, also in both samples. The results are shown in Figs. 4 and 7 as the dotted-dashed line for forbidden LO-phonon scattering [$\mathbf{z}(\mathbf{x},\mathbf{x})\bar{\mathbf{z}}$], and in Fig. 7 as the solid line for constructive [$\mathbf{z}(\mathbf{x}',\mathbf{x}')\bar{\mathbf{z}}$] and the dashed line for destructive interference

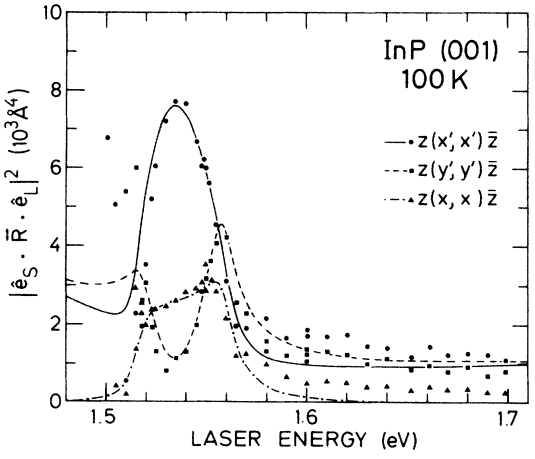

FIG. 7. LO-phonon Raman polarizabilities for the three scattering configurations ($\hat{e}_L||\hat{e}_S$) corrected for the resonance of unknown origin. The lines represent fits to the experimental points. The parameters used for the fits are listed in Table I.

$[\mathbf{z}(\mathbf{y}',\mathbf{y}')\bar{\mathbf{z}}]$ between allowed and forbidden scattering. The parameters used for this fit are listed in Table I. For the sake of completeness we show in Fig. 8 the real and imaginary parts of the Raman polarizabilities a_{DP} and a_F used for this fit. The theoretical fits of Fig. 7 represent the experimental points rather well, thus confirming that our theory adequately describes the interference effects in resonant Raman scattering by one LO phonon and the resonant Raman scattering by two LO phonon. This suggests that excitonic interaction is not important near $E_0+\Delta_0$ in InP at 100 K. Even the maximum in the configuration $\mathbf{z}(\mathbf{y}',\mathbf{y}')\bar{\mathbf{z}}$ at 1.56 eV (outgoing resonance) is well reproduced by the fit, as was not the case for GaAs.[2] A different choice of the broadening parameter η [as described above: 3.5 meV instead of 8 meV (Ref. 37)] might remove this discrepancy in GaAs.

The following similarities between the interference effects in InP and GaAs should be mentioned. The sign of the interference $[\mathbf{z}(\mathbf{x}',\mathbf{x}')\bar{\mathbf{z}}$ constructive interference, $\mathbf{z}(\mathbf{y}',\mathbf{y}')\bar{\mathbf{z}}$ destructive interference] is the same in InP as in GaAs, as predicted by theory. Since $s_e-s_h<0$ in Eq. (9), the real and imaginary parts of the Raman polarizability a_F for LO-phonon forbidden scattering are positive near the resonance maximum, and so is the Raman polarizability a_{DP} for LO-phonon allowed scattering as shown in Fig. 8.[38] Thus, the real and imaginary parts of a_F and a_{DP} have the same sign in InP as in GaAs and the same type of interference is obtained in both materials. Moreover, in high-purity InP, as much as in GaAs,[2] the impurity-induced contribution to the LO-phonon forbidden Raman scattering amounts to about 60%, and thus the investigation of LO-phonon interference effects may provide a good method of characterizing samples in a purity or compensation range where Hall-mobility measurements are of no help.

Our fits also suggest that the LO-phonon Raman scattering resonates near $E_0+\Delta_0$ at a gap 9 meV higher than the two-LO-phonon scattering. This also seems to be the case for LO phonons in GaAs.[37] The fact that different scattering processes may resonate at slightly different electronic gaps has already been pointed out.[39,40] It has been suggested that the electron-phonon interaction may renormalize differently the gaps that enter the dielectric function and the different Raman scattering efficiencies. However, a quantitative theoretical explanation has not yet been given. We note that in Ref. 3 the same values of the $E_0+\Delta_0$ energy were used for the fit of the LO-phonon and two-LO-phonon resonances in CdTe. However, the phonon energy in CdTe (21 meV) is only half that of InP. If the shift in the resonant gap were a fraction of this phonon energy ($\approx\frac{1}{4}$ for InP), it would fall within the experimental uncertainty in the case of CdTe.

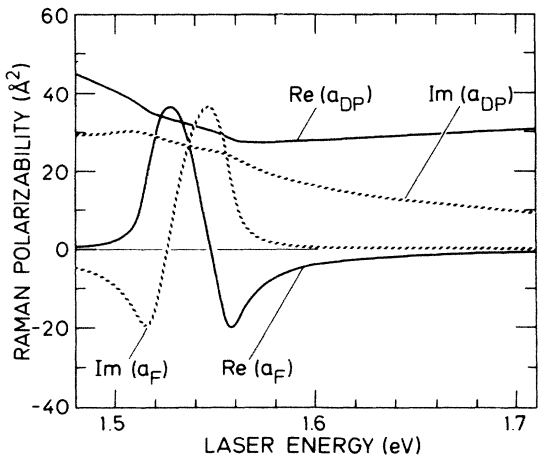

FIG. 8. Energy dependence of the Raman polarizabilities a_{DP} for LO-phonon allowed scattering [Eq. (4)] and a_F for LO-phonon intrinsic forbidden scattering [Eq. (9)] calculated with the parameters used for the fit of Fig. 7.

VI. CONCLUSIONS

We have shown that resonant Raman scattering by two LO phonons can be used to determine the $E_0+\Delta_0$ gap position and its broadening η. We have also demonstrated that allowed and forbidden Raman scattering by one LO phonon interfere in InP in a way similar to that reported for GaAs. The observed interferences can be fitted with the value of η obtained from the two-LO-phonon resonance profile. Even in high-purity InP, we need 60% of impurity-induced incoherent Raman scattering in order to account for the observed interferences in the resonance profiles. The optical deformation potential d_0 determined from the broadening η of the $E_0+\Delta_0$ gap by two-LO-phonon Raman scattering is about 14 eV, more than a factor of 2 lower than that determined by other optical methods.

ACKNOWLEDGMENTS

The authors gratefully acknowledge the help of J. Menéndez, his interest in this work, and his incisive comments. We also wish to express our gratitude to M. Siemers, H. Hirt, and P. Wurster for their technical assistance and to M. Heyen, H. Jürgensen, K. Benz, and F. Scholz for providing the MOCVD samples.

[1]J. Menéndez and M. Cardona, Phys. Rev. Lett. 51, 1297 (1983).
[2]J. Menéndez and M. Cardona, Phys. Rev. B 31, 3696 (1985).
[3]J. Menéndez, M. Cardona, and L. K. Vodopyanov, Phys. Rev. B 31, 3705 (1985).
[4]W. J. Turner, W. E. Reese, and G. D. Pettit, Phys. Rev. 136, A1467 (1964).
[5]J. Camassel, P. Merle, L. Bayo, and H. Mathieu, Phys. Rev. B 22, 2020 (1980).
[6]M. H. Grimsditch, D. Olego, and M. Cardona, Phys. Rev. B 20, 1758 (1979).
[7]M. Cardona, in *Light Scattering in Solids II*, Vol. 50 of *Topics in Applied Physics*, edited by M. Cardona and G. Güntherodt (Springer, Heidelberg, 1982), p. 19.
[8]A. Mooradian and G. B. Wright, Solid State Commun. 4, 431 (1966).
[9]M. Sinyukov, R. Trommer, and M. Cardona, Phys. Status Soli-

di B **86**, 563 (1978).
[10]F. Meseguer, J. C. Merle, and M. Cardona, Solid State Commun. **50**, 709 (1984).
[11]M. Cardona, in *Proceedings of the International School in Physics "Enrico Fermi,"* Course 52, edited by E. Burstein (Academic, New York, 1972), p. 514.
[12]F. Canal, H. Grimsditch, and M. Cardona, Solid State Commun. **29**, 523 (1979).
[13]P. J. Colwell and M. V. Klein, Solid State Commun. **8**, 2095 (1970); A. A. Gogolin and E. I. Rashba, in *Proceedings of the 13th International Conference on the Physics of Semiconductors, Rome,* edited by F. G. Fermi (Tipographia Marves, Rome, 1976), p. 284; A. A. Gogolin and E. I. Rashba, Solid State Commun. **19**, 1177 (1976).
[14]R. Zeyher, Phys. Rev. B **9**, 4439 (1974).
[15]A. A. Klochikhin and A. G. Plyukhin, Pis'ma Zh. Eksp. Teor. Fiz. **21**, 265 (1975) [JETP Lett. **21**, 122 (1975)].
[16]A. A. Klochikhin, S. A. Permogorov, and A. N. Reznitskii, Zh. Eksp. Teor. Fiz. **71**, 2230 (1976) [Sov. Phys.—JETP **44**, 1176 (1976)].
[17]A. A. Abdumalikov and A. A. Klochikhin, Phys. Status Solidi B **80**, 43 (1977).
[18]A. A. Klochikhin, Ya. V. Morozenko, and S. A. Permogorov, Fiz. Tverd. Tela (Leningrad) **20**, 355 (1978) [Sov. Phys.—Solid State **20**, 2057 (1978)].
[19]P. Lawaetz, D.Sc. thesis, The Technical University of Denmark, Lyngby, 1978.
[20]A. Blacha, H. Presting, and M. Cardona, Phys. Status Solidi B **126**, 11 (1984).
[21]H. C. Gatos and M. C. Lavine, in *Progress in Semiconductors,* edited by A. F. Gibson and R. E. Burgess (Temple, London, 1965), Vol. 9, p. 1.
[22]H. C. Gatos and M. C. Lavine, J. Electrochem. Soc. **107**, 427 (1960).
[23]J. Wagner and M. Cardona, Solid State Commun. **48**, 301 (1983).
[24]W. C. Dash and R. Newman, Phys. Rev. **99**, 1151 (1955).
[25]D. E. Aspnes and A. A. Studna, Phys. Rev. B **27**, 985 (1983).
[26]D. E. Aspnes and J. E. Rowe (unpublished), quoted in Ref. 19.
[27]H. Presting, Ph.D. thesis, Universität Stuttgart, 1985.
[28]J. D. Wiley, in *Semiconductors and Semimetals,* edited by R. K. Willardson and A. C. Beer (Academic, New York, 1975), Vol. 10, p. 91.
[29]N. E. Christensen, Phys. Rev. B **30**, 5753 (1984).
[30]N. E. Christensen (private communication).
[31]D. D. Sell (unpublished), quoted in Ref. 19. Unfortunately, the data used for this determination, like those used by Lawaetz (Ref. 19) for similar determinations in other zinc-blende-type compounds, have remained unpublished and thus cannot be reexamined.
[32]N. E. Christensen, Solid State Commun. **50**, 177 (1984).
[33]O. H. Nielsen (private communication).
[34]D. D. Sell and S. E. Stokowski, in *Proceedings of the 10th International Conference on the Physics of Semiconductors, Cambridge, Mass.,* edited by S. P. Keller, J. C. Hensel, and F. Stern (U.S. AEC, Oak Ridge, 1970), p. 417.
[35]M. Reine, R. L. Aggarwal, B. Lax, and C. H. Wolfe, Phys. Rev. B **2**, 458 (1970).
[36]D. E. Aspnes and A. A. Studna, Phys. Rev. B **7**, 4605 (1973).
[37]W. Kauschke and M. Cardona (unpublished).
[38]Note that a positive C_F implies, for the choice of axes given in Sec. III, that the dynamical charge e_T is negative at the anion (Ref. 2).
[39]M. A. Renucci, J. B. Renucci, R. Zeyher, and M. Cardona, Phys. Rev. B **10**, 4309 (1974).
[40]W. Kiefer, W. Richter, and M. Cardona, Phys. Rev. B **12**, 2346 (1975).
[41]E. Matatagui, A. G. Thompson, and M. Cardona, Phys. Rev. **176**, 950 (1968).
[42]E. D. Palik and R. F. Wallis, Phys. Rev. **123**, 131 (1961).
[43]P. Rochon and E. Fortin, Phys. Rev. B **12**, 5803 (1975).
[44]I. Kudman and R. J. Pfaff, J. Appl. Phys. **43**, 3760 (1972).
[45]M. Hass and B. W. Henvis, J. Phys. Chem. Solids **23**, 1099 (1962).